Rigorous characterization of time-resolved diffuse spectroscopy systems for measurements of absorption and scattering properties using solid phantoms

Swartling, Johannes; Pifferi, Antonio; Giambattistelli, Eleonora; Chikoidze, Ekaterine; Torricelli, Alessandro; Taroni, Paola; Andersson, Magnus; Nilsson, Anders; Andersson-Engels, Stefan

Published in:
Proceedings of SPIE - The International Society for Optical Engineering

DOI:
10.1117/12.500580

2003

Rigorous characterization of time-resolved diffuse spectroscopy systems for measurements of absorption and scattering properties using solid phantoms

Johannes Swartling[1], Antonio Pifferi[2], Eleonora Giambattistelli[2], Ekaterine Chikoidze[2], Alessandro Torricelli[2], Paola Taroni[2], Magnus Andersson[1], Anders Nilsson[1], Stefan Andersson-Engels[1]

[1]*Department of Physics, Lund Institute of Technology, P.O. Box 118, SE-221 00 Lund, Sweden*
johannes.swartling@fysik.lth.se

[2]*INFM-Dipartimento di Fisica and IFN-CNR, Politecnico di Milano, Piazza Leonardo da Vinci 32, 20133 Milan, Italy*
antonio.pifferi@fisi.polimi.it

ABSTRACT

Two systems for measurements of absorption and scattering properties, based on picosecond-pulse lasers and single-photon counting detection, were characterized using a detailed protocol. The first system utilizes diode lasers at 660, 785, 910 and 974 nm as light sources. The second employs a Ti:sapphire and a mode-locked dye laser to produce tunable pulses in the range 610 – 1000 nm. Using solid tissue phantoms, the systems were rigorously characterized and compared in terms of absolute accuracy of the measured scattering and absorption coefficients, the linearity over the parameter range, the precision with respect to injected light energy, the stability over time, and the reproducibility of the results. The phantoms were made of epoxy resin with TiO as scatterer and black toner powder as absorber.

Keywords: time-resolved, photon migration, diffusion equation, phantoms

INTRODUCTION

Accurate measurements of the absorption coefficient μ_a, and the reduced scattering coefficient μ_s', in turbid media have become important in the research of new diagnostic modalities based on photon migration. When developing imaging techniques, reference techniques are necessary that can measure the local optical properties over small sampling volumes, where μ_a and μ_s' can be assumed to be constant. Spectroscopic *in-vivo* measurements of this kind are now routinely performed to determine the parameter range of μ_a and μ_s' for various types of healthy and diseased tissues. Since the results serve as a basis for further development, it is important the values are representative of the "true" properties of the tissue, and that the variance and possible systematic errors in the measurements are well known.

The measurement techniques employed are usually either based on frequency-modulated light sources,[1] or time-resolved diffuse spectroscopy.[2] In this work, we have investigated two time-resolved systems using a detailed protocol, involving measurements on a set of solid tissue phantoms made of epoxy resin. The absorption and reduced scattering coefficients were determined from the measurements with the assumption of a homogeneous medium. Previous phantom studies have concluded that the *accuracy* of the time-resolved technique is better than 10% for $\mu_a < 1$ cm^{-1} and $\mu_s' > 10$ cm^{-1}.[2] Here, we extend the protocol for characterization of the measurement technique to include an evaluation of the *linearity* of the results over the parameter range of interest. The third point is to assess the *precision* of the measurements in terms of the sensitivity with respect to the injected light energy during the recording. Finally, the *stability* of the results over time, and their *reproducibility* between measurement sessions, are also evaluated.

Photon Migration and Diffuse-Light Imaging, David A. Boas, Editor,
Proceedings of SPIE-OSA Biomedical Optics, SPIE Vol. 5138 (2003)

MATERIALS AND METHODS

Diode-laser based time-resolved system

The first system, henceforth called the "diode laser system," is a portable system constructed at the Lund Medical Laser Centre, Lund, Sweden. The system, schematically depicted in Fig. 1, was designed with the primary objective to perform *in-vivo* measurements of the optical properties in a clinical environment, and specifically the oxygen saturation of the tissue. Moreover, measurements are carried out using relatively small inter-fiber distances, $\rho < 2$ cm, to enable small sampling volumes. This means that the instrument response function (IRF) of the system must be short, with a full width at half maximum (FWHM) of less than 100 ps. In addition, it means that the average laser power can be kept relatively low, around 2 mW, and the light collection of the detection system does not require the use of thick fiber bundles. As light sources, diode lasers at 660, 785, 910 or 974 nm could be used, driven by a SEPIA controller (PicoQuant GmbH, Germany). The light was guided to the sample using 200-μm gradient index fibers. A simple probe was constructed, which enabled diffuse reflectance measurements at different ρ by means of linear translation of the source and detection fibers. To collect the light, a 600-μm gradient index fiber was used. A cooled microchannel-plate photomultiplier (MCP-PMT) (R2566U, Hamamatsu Photonics K.K., Japan) was used for detection. The system utilizes the time-correlated single-photon counting (TCSPC) technique to obtain the temporal point-spread function (TPSF)[3]. An SPC-300 computer card (Becker & Hickl GmbH, Germany) provides the electronics for the TCSPC detection, and the system is controlled from a flat panel PC with a touch-sensitive screen. The FWHM of the instrument response function (IRF) for the detection part was approximately 30 ps, and the width of the laser pulses was about 70 ps when the output intensity after the fiber was kept below 2 mW. This resulted in a total IRF of < 100 ps.

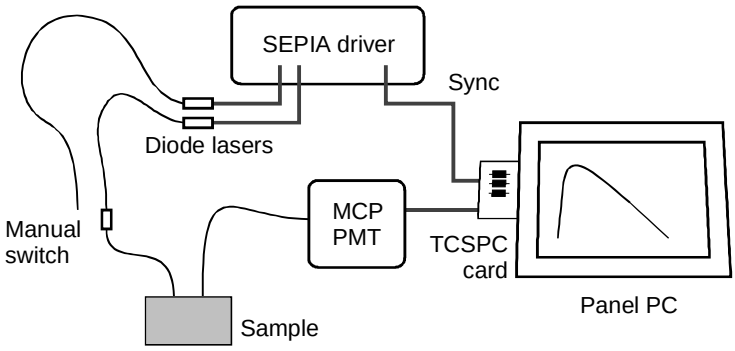

Fig. 1 Schematic picture of the diode laser system.

Fully spectroscopic time-resolved system

The second system, henceforth called the "spectroscopy system," is based on wavelength scanning of tunable mode-locked lasers. Figure 2 shows the scheme of the system set-up. A synchronously-pumped mode-locked dye (DCM) laser was used as the excitation source from 610 to 695 nm, while an actively mode-locked Titanium:Sapphire laser provided light in the wavelength range of 700 to 1000 nm. A 1.0-mm plastic-glass fiber (PCS1000W, Quartz et Silice, France) delivered light into the tissue, while diffusely reflected photons were collected by means of a 5 mm diameter fiber bundle. The power density at the distal end of the illumination fibre was always limited to less than 10 mW. A home-built caliper allowed us to position the fibres at the relative distance of 1.5 – 4 cm, parallel to each other and normal to the tissue surface. A cooled MCP-PMT (R1564U with S1 photochatode, Hamamatsu Photonics K.K., Japan) and an electronic chain for TCSPC were used for detection. A small fraction of the incident beam was coupled to a 1.0 mm fiber (PCS1000W, Quartz et Silice, France) and fed directly to the photomultiplier to account for on-line recording of the IRF. Overall, the IRF was <120 ps and <180 ps FWHM in the red and near-infrared, respectively.

Time-resolved reflectance curves were collected every 5 nm from 610 to 1000 nm. In order to allow measurements to be carried out *in vivo*, the system for the acquisition of time-resolved data was fully automated and the analysis and display of the measured spectra were performed in real time. A PC controlled the laser tuning and power, the monochromator

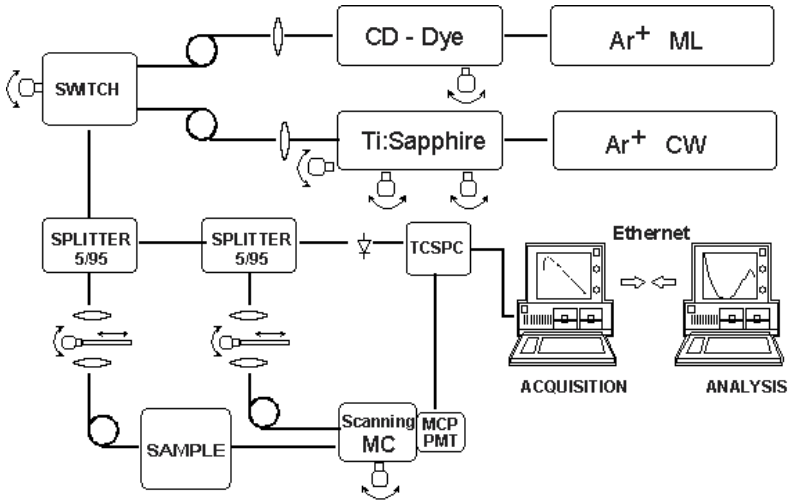

Fig. 2 Schematic picture of the spectroscopy system.

scanning, and the optimisation of the IRF, by automatically adjusting the laser cavity length. The overall measurement time (for data acquisition and system adjustment) was 5 s/wavelength.

Evaluation of time-resolved data

The absorption and transport scattering coefficients, μ_a and μ_s', respectively, were obtained by fitting the solution of the diffusion equation for a semi-infinite homogenous medium with the extrapolated boundary condition to the measured data[4]. The diffusion coefficient, *D*, was assumed to be independent of the absorption of the medium, *i.e.*, $D = 1/3\mu_s'$.[5] The theoretical curve was convolved with the IRF. The resulting curve was fitted to the data over a range starting at 80% of the maximum intensity on the rising flank and ending at 1% on the trailing flank.[6] The fit was performed with a Levenberg-Marquardt algorithm by varying μ_a and μ_s' in order to minimize χ^2.[7] The same software was used for evaluation of data for both systems.

Solid tissue phantoms

A set of 25 phantoms was prepared from clear, solvent-free epoxy resin (NM 500, Nils Malmgren AB, Ytterby, Sweden), according to the guidelines given by Firbank et al.[8,9]. As scatterer, TiO powder was used (Sigma-Aldrich, T-8141). As absorbing pigment, toner from the copying machine was used, which had a fairly flat absorption spectrum throughout the visible and NIR region. The toner also had some scattering characteristics, which means that, unfortunately, the absorption coefficient is not trivially obtained from spectrophotometer readings alone. The concentrations of TiO and absorbing pigment are shown in Table 1. The concentrations were selected to reflect a range of μ_a and μ_s' typical of biological tissues. Cylindrical polypropylene cups were used as molds, resulting in phantoms with a diameter of 6.5 cm and a height of 5.5 cm. After hardening, the upper surface was machined smooth. To provide independent validation of the scattering and absorption properties of the phantoms, an integrating sphere set-up was

Table 1. Concentration of TiO and black pigment added to the phantoms

Phantom (increasing μ_s')	TiO (mg/g)		Phantom (increasing μ_a)	Black pigment (μg/g)
A	0.79		1	6.4
B	1.20		2	13.8
C	1.61		3	21.1
D	2.02		4	28.5
E	2.42		5	35.9

used[10,11]. For the integrating sphere measurements, cuvettes were made of microscope slides into which about 1 ml from each phantom was poured before the epoxy hardened.

Protocol for characterization of the two systems

The measurement protocol to characterize the systems consists of five parts, where the first involves determination of the absolute *accuracy* of the measured values. Next, the *linearity* of the results over the parameter range of interest is evaluated. The third point is to assess the *precision* of the measurements in terms of the sensitivity with respect to the injected light energy during the recording. Finally, the *stability* of the results over time, and their *reproducibility* between measurement sessions, are evaluated. It should be noted that these points apply to the entire process of determining the optical properties, and thus also depend on the evaluation model used to deduce the scattering and absorption coefficients from the time-resolved data. The system is in this respect viewed as a "black box," where the measurement data are acquired at one end, and the resulting optical properties are obtained at the other. This makes the protocol versatile and useful for any system, from pure research set-ups to commercial instruments. However, the implications of the various parts of the process for determining the optical properties will also be discussed in this paper.

For the measurements of accuracy, linearity, stability and reproducibility, the acquisition time was adjusted so that at least 100 000 counts were collected for each TPSF curve. This represented the minimum desired number of counts during realistic *in-vivo* measurements. Depending on the optical properties of the sample, this meant acquisition times, per TPSF curve, ranging from a few seconds up to a few minutes for the diode laser system at the maximum inter-fiber distance and scattering and absorption coefficients. To determine the absolute accuracy, the whole set of 25 phantoms was measured with the diode laser system. For the spectroscopy system, due to the longer time required to acquire a whole spectrum, 3 scattering series out of 5 were measured, for a total of 15 samples. Thus, the phantoms B1 – B5 and D1 – D5 (cf. Table 1) were excluded from the investigation with this system. To reflect the optimal inter-fiber distances that each system was designed for, using the diode laser system, $\rho = 1.5$ cm, and using the spectroscopy system, $\rho = 2.0$ cm.

In the next part of the protocol, the precision of the measurements was evaluated by measuring at different amounts of injected light energy per measurement. To this end, a set of 3000 repeated measurements were performed, each 0.1 s long, on one sample (C1, according to Table 1). The inter-fiber distances were $\rho = 1.5$ cm for the diode laser system, and $\rho = 2.0$ cm for the spectroscopy system, to reflect the normal working conditions for each system. These measurements each represented the lowest value of injected energy per measurement. The coefficients μ_a and μ_s' were evaluated for each of the measurements in the set, and then the coefficient of variation (*CV*) for the results was calculated as

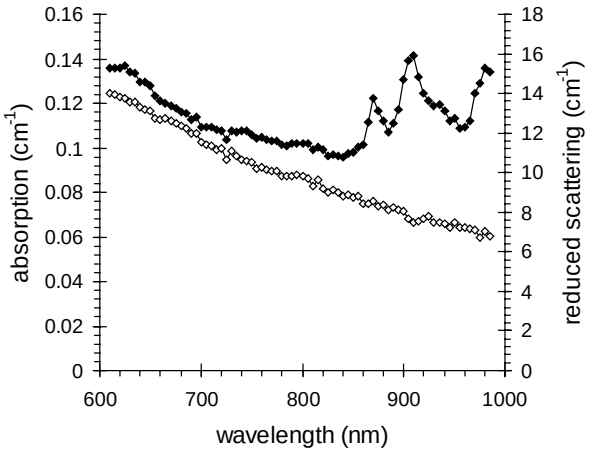

Fig. 3 Absorption and scattering spectrum of phantom C2, measured with the spectroscopy system.

$$CV = \frac{\sigma}{< x >}$$

where σ is the standard deviation and $< x >$ is the mean of either μ_a or μ_s'. In the next step, the measurements were paired, and the average of each pair taken to form a new set, representing twice the value of injected energy per measurement, and new values of μ_a, μ_s', and *CV* were calculated. This procedure was repeated for increasing values of injected energy, doubling in each step.

For the next step, the stability of the measurements over time was evaluated. Repeated measurements were performed over a period of 2 hours, to investigate any drift in the systems.

Finally, the reproducibility of the measurements was assessed by repeating measurements on the same phantom, with identical measurement parameters, every day for 5 days.

RESULTS

An example of the spectral characteristics of the solid phantoms, measured with the spectroscopy system, is presented in Fig. 3. The peaks in the absorption spectrum around 900 nm stems from the epoxy. Below 800 nm, the epoxy absorption has been reported to be fairly flat at 0.01 cm^{-1},[9] so most of the absorption in this region is due to the black pigment. The determined values of μ_a and μ_s' for both systems, at 660 nm, are presented in Fig. 4. The values for μ_s' from the integrating sphere meaurements are also shown for comparison.

Results for the linearity in μ_a are presented in Fig. 5, for both systems, with ρ = 1.5 cm for the diode laser system, ρ = 2 cm and for the spectroscopy system. The absorption coefficients are shown as function of the concentration of black pigment, evaluated at 660 nm, for the phantoms with lowest (row A) and highest (row E) scattering coefficient, respectively. The linearity in scattering is presented in Fig. 6, for the phantoms with lowest (row 1) and highest (row 5) absorption coefficient, respectively. The lowest values of scattering (row A) were left out when calculating the regression line in Fig. 6 (a). The results were similar for the evaluation of the diode laser system at 10 mm (data not

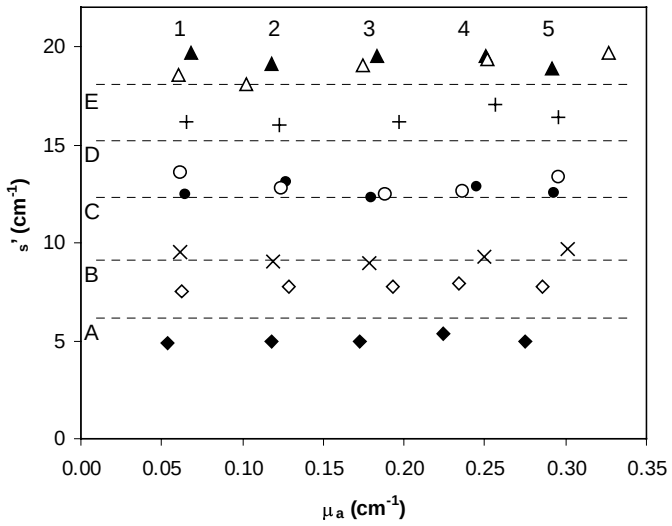

Fig. 4 Values of absorption and scattering coefficients of the phantoms, at 660 nm, evaluated with both systems. Filled and crossed symbols are for the diode laser system, and empty symbols are for the spectroscopy system. Note that rows B and D for scattering were not measured with the spectroscopy system, so the data shown are for rows A, C and E for this system. The dashed lines represent the average values from the integrating sphere measurements for rows A – E. Absorption data from the integrating sphere is not shown.

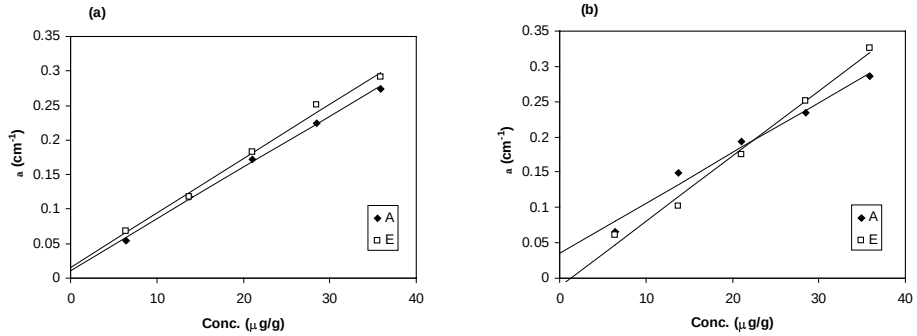

Fig. 5 Linearity test showing the absorption coefficient as a function of the concentration of black pigment in the phantoms. Data are shown for rows A and B, according to Table 1. (a) The diode laser system. (b) The spectroscopy system.

shown). Since only three scattering concentrations were measured using the spectroscopy system, it is difficult to evaluate the linearity in this case, but the data in Fig. 6 (b) is included for completeness.

The results from the evaluation of precision on the estimate of μ_a using the spectroscopy system operated at 660 nm are presented in Fig. 7 as a function of the injected energy. These data were obtained on the phantom C2 with an interfiber distance of 2 cm. Similar results were derived for the estimate of μ_s'.

The evaluation of the stability over time of the systems revealed that no drift was apparent when performing measurements over a period of 2 hours. During the measurement series, the only varition in the readings was the stochastic variation as shown in Fig. 7. Finally, the reproducibility measurements, taken every day over 5 days, showed a slightly higher standard deviation, but the *CV* was in all cases less than 5%.

DISCUSSION

In terms of absolute accuracy of the determined values of μ_a and μ_s', some problems are associated with the solid phantoms. The exact properties of the phantoms are unknown, although the independent integrating sphere measurements likely give values of μ_s' that are within 5% accurate. Integrating sphere measurements are less accurate for the absorption coefficient, but it is reasonable to assume that the true absorption is linearly related to the concentration of black pigment. When preparing the phantoms, much care was taken to mix the resin, TiO, and black pigment, both mechanically and using an ultrasonic bath, and it is unlikely that there were significant inhomogeneities in

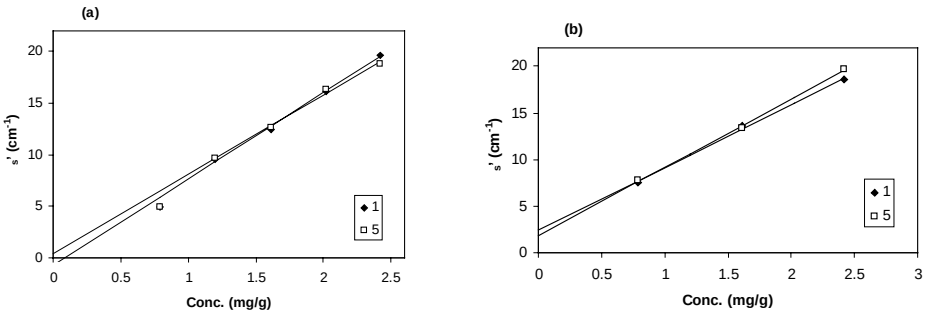

Fig. 6 Linearity test for the scattering coefficient as a function of the concentration of TiO in the phantoms. Data are shown for rows 1 and 5, according to Table 1. (a) Diode laser system. Note that the data points for the lowest scattering were left out of the calculation of the regression line. (b) Spectroscopy system.

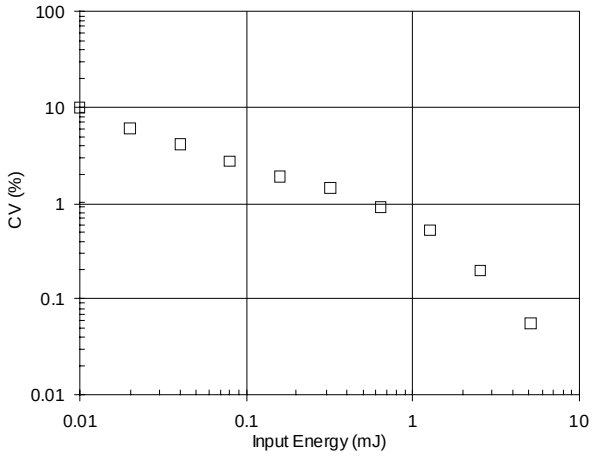

Fig. 7 Results from the precision measurement, showing *CV* on μ_a for the spectroscopy system as a function of the input energy during the recording. The count rate was 100 000 counts/s during the measurement. The curve for μ_s' was similar.

the phantoms. The results presented in Fig. 4 indicate that the accuracy for both systems is better than 10% within the parameter range defined the B – C phantoms, but slightly worse for the low-scattering A phantoms.

With respect to linearity, from Fig. 5, it is apparent that the evaluation of μ_a was linear over the entire parameter range. Turning the attention to the scattering coefficient, the expected linear behavior of μ_s' deviates slightly for the lowest concentration of scatterer. This may be the result of entering the regime where the diffusion approximation used in the evaluation is no longer entirely valid, i.e., the detection position cannot be regarded as far away from the source. The conclusion is that μ_a was linear over the entire range up to 0.3 cm^{-1}, while μ_s' was linear for $\mu_s' > 9$ cm^{-1}, with an error <30% at 6 cm^{-1}.

In the next part, the precision of the measurements was investigated in terms of *CV* for various levels of injected energy per measurement, as presented in Fig. 7. For time-resolved instruments, *CV* is largely determined by the number of counts in the TPSF, *N*, primarily due to the noise, which is proportional to $N^{1/2}$. The contribution of noise by the dark current in the detectors was negligible for both systems. Translated to injected energy per measurement, the relationship with *N* is dependent on the average power, the collection efficiency and sensitivity of the detection system, the inter-fiber distance, and the properties of the sample. The conclusion of the precision evaluation is that an input energy of 1 mJ on the phantom C2 (μ_a = 0.12 cm^{-1}, μ_s' = 12 cm^{-1}) yields a CV of 1%, that is acceptable for most applications. This corresponds to an acquisition time of 1 s using an incident power of 1 mW, and produces about 100,000 counts on the whole time dispersion curve.

The stability results revealed no drift in any of the systems. TCSPC measurements are largely insensitive to drift in the intensity of the laser pulses, but temporal shifts can cause problems if the IRF is not monitored simultaneously with the measurements. On-line monitoring of the IRF was performed for the spectroscopy system, but not for the diode laser system. In this test, no drift was apparent in the diode laser system, but nevertheless, we recommend that on-line measurements of the IRF are carried out.

The final part of the solid-phantom protocol was the reproducibility of the results. It was evident that *CV* < 5% for measurements performed under identical conditions on different days. The conclusion is that reproducibility is not a limiting factor as far as the instrumentation is concerned.

CONCLUSIONS

In conclusion, two time-domain diffuse spectroscopy systems were characterised in terms of accuracy, linearity, precision, stability and reproducibility. The results show that the systems were capable of determining the absorption and reduced scattering coefficient with an accuracy of 10% within the parameter range $9 < \mu_s' < 20$ cm^{-1} and $0 < \mu_a < 0.3$ cm^{-1}. For lower scattering, down to 6 cm^{-1}, the relative error in μ_s' was slightly worse at about 20 – 30%. The precision of the measurements was better than 1% if 100 000 counts per TPSF curve were acquired. In terms of stability, no drift in the readings was detected, and the day-to-day reproducibility was better than 5%.

ACKNOWLEDGEMENTS

This work was partially supported by the European Commission grants HPRI-CT-2001-00148, QLG1-CT-2000-00690 (OPTIMAMM), QLG1-CT-2000-01464 (MEDPHOT). E. Chikoidze acknowledges support by the TRIL programme, Trieste, Italy.

REFERENCES

1. S. J. Madsen, E. R. Anderson, R. C. Haskell, and B. J. Tromberg, "Portable, high-bandwidth frequency-domain photon migration instrument for tissue spectroscopy," Opt. Lett. **19,** 1934-1936 (1994).
2. R. Cubeddu, M. Musolino, A. Pifferi, P. Taroni, and G. Valentini, "Time resolved reflectance: a systematic study for the application to the optical characterization of tissue," IEEE J. Quant. Electr. **30,** 2421-2430 (1994).
3. S. Andersson-Engels, R. Berg, O. Jarlman, and S. Svanberg, "Time-resolved transillumination for medical diagnostics," Opt. Lett. **15,** 1179-1181 (1990).
4. R. C. Haskell, L. O. Svaasand, T.-T. Tsay, T.-C. Feng, M. S. McAdams, and B. J. Tromberg, "Boundary conditions for the diffusion equation in radiative transfer," J. Opt. Soc. Am. A **11,** 2727-2741 (1994).
5. K. Furutsu and Y. Yamada, "Diffusion approximation for a dissipative random medium and the applications," Phys. Rev. E **50,** 3634-3640 (1994).
6. R. Cubeddu, A. Pifferi, P. Taroni, A. Torricelli, and G. Valentini, "Experimental test of theoretical models for time-resolved reflectance," Med. Phys. **23,** 1625-1633 (1996).
7. W. H. Press, S. A. Teukolsky, W. T. Vetterling, and B. P. Flannery, *Numerical recipes in C: The art of scientific computing*, (Cambridge University Press, New York, 1992).
8. M. Firbank and D. T. Delpy, "A design for a stable and reproducible phantom for use in near infra-red imaging and spectroscopy," Phys. Med. Biol. **38,** 847-853 (1993).
9. M. Firbank, M. Oda, and D. T. Delpy, "An improved design for a stable and reproducable phantom material for use in near-infrared spectroscopy and imaging," Phys. Med. Biol. **40,** 955-961 (1995).
10. A. M. K. Nilsson, R. Berg, and S. Andersson-Engels, "Measurements of the optical properties of tissue in conjunction with photodynamic therapy," Appl. Opt. **34,** 4609-4619 (1995).
11. J. Swartling, J. S. Dam, and S. Andersson-Engels, "Comparison of spatially and temporally resolved diffuse-reflectance measurement systems for determination of biomedical optical properties," Appl. Opt. In press (2003)